Exploration of the Behaviour of a Stochastic Transport Model Using Computational Experiments

C. Rajanayaka and D. Kulasiri

Centre for Advanced Computational Solutions (C-fACS), Applied Management and Computing Division
Lincoln University, Canterbury, New Zealand (rajanayc@lincoln.ac.nz)

Abstract: Fickian assumptions are used in deriving the advection-dispersion equation which models the solute transport in porous media. The hydrodynamic dispersion coefficient defined as a result of these assumptions has been found to be scale dependent. Kulasiri and Verwoerd [1999] developed a stochastic computational model for solute transport in saturated porous media without using Fickian assumptions. The model consists of two main parameters; correlation length and variance, and the velocity of solute was assumed as a fundamental stochastic variable. In this paper, the stochastic model was investigated to understand its behaviour. As the statistical nature of the model changes with the parameters, the computational solution of the model was explored in relation to the parameters. The variance is found to be the dominant parameter, however, there is a correlation between two parameters and they influence the stochasticity of the flow in a complex manner. We hypothesised that the variance is inversely proportional to the pore size and the correlation length represents the geometry of flow. The computational results of different scales show that the hypotheses are reasonable. The model illustrates that it could capture the scale dependence of dispersivity and mimic the advection-dispersion equation in more deterministic situations.

Keywords: Groundwater; Solute Transport; Stochastic Model; Scale Dependence

1. INTRODUCTION

The applied groundwater forecasting and management problems largely rest on formulation of mathematical models. Most of the models, which are commonly used by the practitioners, represent linear time dependent partial differential equations mainly based on deterministic consideration. However, real world aquifer systems consist of heterogeneous formation of porous media, complex boundaries and random distribution of parameters with irregular inputs (rainfall). The complexities of groundwater systems, therefore, cannot be accurately understood by deterministic description and need to be described by stochastic sense such as stochastic differential equations [Unny, 1989]. After the pioneering work of Freeze [1975], various aspects of heterogeneous formations of groundwater systems have been investigated in the past by using stochastic models. Gelhar et al. [1979], Dagan [1984, 1988], Neuman et al. [1987], Russo [1993] and Foussereau et al. [2000] are a few to name among a large number of contributors.

Kulasiri and Verwoerd [1999] developed a stochastic solute transport model (SSTM) assuming the velocity of solute as a fundamental stochastic variable;

$v(x,t)=\bar{v}(x,t)+\xi(x,t)$, where $\bar{v}(x,t)$ = average velocity described by Darcy's law and $\xi(x,t)$ = white noise correlated in space and δ - correlated in time. This model avoids the use of the Fickian assumption that gives rise to the dispersion coefficient, *D*, that proved to be scale dependent [Gelhar, 1986; Fetter, 1999].

In this paper, SSTM was investigated for simple settings of one-dimensional case to understand its behaviour. The computational solution of SSTM was explored in relation to the model parameters. Further, we attempted to relate the model parameters to the real world physical phenomenon.

2. STOCHASTIC MODEL

A detail description the stochastic model can be found in Kulasiri and Verwoerd [1999 and 2001], and brief introduction is given here that enables the

reader to easily refer to the essential components of the model. As shown earlier, when the velocity is described as a stochastic quantity, the formulation of SSTM can be expressed by the following stochastic differential equation;

$$dC = S(\bar{v}(x,t)C(x,t))\,dt + S(C(x,t)\,d\beta(t)), \quad (1)$$

where C = solute concentration,

$\bar{v}$ = mean velocity,

$$d\beta_m(t) = \sum_{j=1}^{m} f_j \sqrt{\lambda_j}\, db_j(t), \quad (2)$$

m = number of terms used,

$db_j(t)$ = increments of standard Wiener processes,

f_j = eigenfunctions of velocity covariance function,

λ_j = eigenvalues of velocity covariance function,

$S = -\left(\frac{h_x}{2}\frac{\partial^2}{\partial x^2} + \frac{\partial}{\partial x}\right)$ is an operator in space and

$h_x = dx$.

An exponential covariance kernel was assumed based on plausible arguments to model the spatial correlation of the noise component of the velocity function, and that can be given by

$$q(x_1, x_2) = \sigma^2 e^{\frac{-y}{b}}, \quad (3)$$

where $y = |x_1 - x_2|$,

b = correlation length, and

σ^2 = variance.

x_1 and x_2 are any two points within the spatial range, $[0, a]$, considered. The eigenfunctions, f_n and eigenvalues, λ_n of $q(x_1, x_2)$ are obtained as the solution to the following integral equation:

$$\int_0^a q(x_1, x_2)\, f_n(x_2)\, dx_2 = \lambda_n f_n(x_1). \quad (4)$$

Assuming σ^2 is a constant over $[0, a]$, the solution to (4) can be obtained by:

$$\lambda_n = \frac{2\theta\sigma^2}{\omega_n^2 + \theta^2}, \quad (5)$$

where $\theta = 1/b$ and ω_ns are the roots of the following equation:

$$\tan \omega_n a = \frac{2\omega_n \theta}{\omega_n^2 - \theta^2}. \quad (6)$$

The basic function of (2) can be obtained by solving (4). The n^{th} basis function is given by

$$f_n(x) = \frac{1}{\sqrt{N}}\left(\sin \omega_n x + \frac{\omega_n}{\theta}\cos \omega_n x\right), \quad (7)$$

where $N = \frac{1}{2}a\left(1 + \frac{\omega^2}{\theta^2}\right) - \frac{1}{4\omega}\left(1 + \frac{\omega^2}{\theta^2}\right)\sin 2\omega a - \frac{1}{2\theta}(\cos 2\omega a - 1)$. (8)

3. COMPUTATIONAL INVESTIGATION

SSTM was investigated for simple settings of one-dimensional case to understand its behaviour. The main parameters of the model are the correlation length, b and the variance, σ^2. As the statistical nature of the computational solution changes with different b and σ^2, the main objective of this exercise is to identify effect of these parameters to the solution of the model.

Distributed concentration values of (1) were obtained by using the finite difference numerical solution taking the numerical convergence and stability into account. We first illustrate the behaviour of the model by solving one-dimensional problem for the spatial domain of 1 m ($0 \le x \le 1$). We solved (6) to generate the roots for a given set of parameters. For an instance, for the correlation length, b = 0.1 m we obtained 29 roots: ω_1 = 2.62768, ω_2 = 5.30732, ω_3 = 8.06714, ……, ω_{29} = 88.1904. Generally 29 terms are more than sufficient to produce converging numerical solution. We generated the standard Wiener process increments in Hilbert space for the time intervals of 0.001 days for total time of 3 days. Then eigenvalues λ_n of (5) were computed for required σ^2. With these roots, ω and λ_n, we calculated the basic function (7). Those values were used to generate $d\beta(t)$ in (2). The numerical scheme of SSTM was then used to calculate the concentration profile for spatial-temporal development for the mean velocity of 0.5 m/day.

We used spatial grid length of 0.1m for the numerical calculation. Initial concentration value of 1.0 unit was considered at x = 0 and it was assumed as a continuous source for the entire time period of the solution. Exponentially distributed point source concentration values at $e^{-5k\,\Delta x}$, where k = 1, 2, …,10 and Δx = grid size, were considered as the initial conditions of other spatial coordinates.

To investigate the general behaviour of the model, we obtained the temporal development of the concentration profiles at the mid point of the domain (x = 0.5m) for various parameter combinations of b and σ^2. The same realisation of

standard Wiener process increments and constant mean velocity of 0.5 m/day were used for all the computational experiments.

First we illustrate that SSTM can mimic the solution of advection-dispersion equation. We used the concentration values of the stochastic model to estimate the appropriate *D* of advection-dispersion model by using a stochastic inverse method [Rajanayaka et al., 2001]. The parameters of SSTM, σ^2 = 0.001 and *b* = 0.0001, gave the corresponding estimate of 0.01 m^2/day for *D*. SSTM can represent the advection-dispersion model with the estimated *D* (Figure 1).

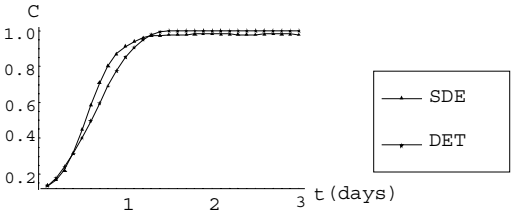

Figure 1. Comparison of deterministic (*D*=0.01) and stochastic (σ^2 = 0.001 and *b* = 0.0001) model concentration profiles for 1 m domain.

Figure 2 illustrates that SSTM could mimic the advection-dispersion model even for a larger scale, $0 \le x \le 10$ m, for 30 day time period. We used the same SSTM parameters that were used in 1 m case and obtained the estimate of 0.037 m^2/day for *D*.

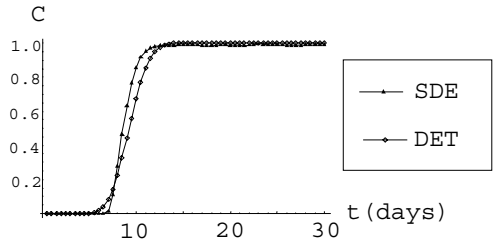

Figure 2. Comparison of deterministic (*D*=0.037) and stochastic (σ^2 = 0.001 and *b* = 0.0001) model concentration profiles for 10 m domain.

We explored the changes of the statistical nature of the model with different *b* and σ^2. The behavioural change of the concentration breakthrough curves was examined by keeping one parameter at a constant and changing the other. Figure 3 shows the concentration profile at *x* = 0.5m of 1 m domain, for a smaller value of σ^2 (0.0001) when *b* varies from 0.0001m to 0.25m. The stochastic behaviour of almost all five curves are insignificant. Even with the help of the legend, it is difficult to distinguish the different profiles. Although, range of *b* varies from 0.0001to 0.25m (a change of 2500 times) the change of stochasticity is negligible for smaller σ^2. When σ^2 approaches 0, flow is advective and the dispersion is negligible.

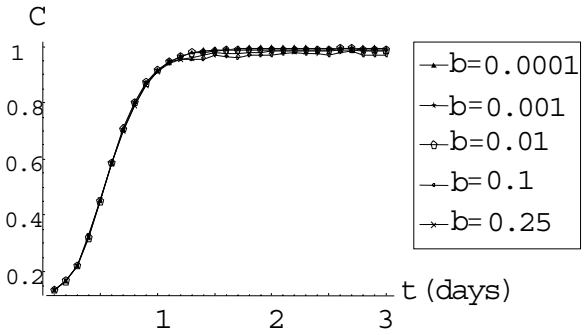

Figure 3. Concentration profile at *x* = 0.5m for σ^2 = 0.0001.

With the increase of σ^2 by 10 times for the same regime of *b* (0.0001m to 0.25m), Figure 4 shows visually distinguishable differences between concentration breakthrough curves. Furthermore, we can observe some curves have undergone notable stochasticity, especially when *b* = 0.1m. The high values of variance not only directly increase the stochastic nature of the flow but also influence the ways in which *b* affects the flow. Another observation we can make from Figure 4 is that with the increase of stochasticity the concentration profile reaches its asymptotic value (sill) early and the maximum concentration value is less than the more deterministic profiles.

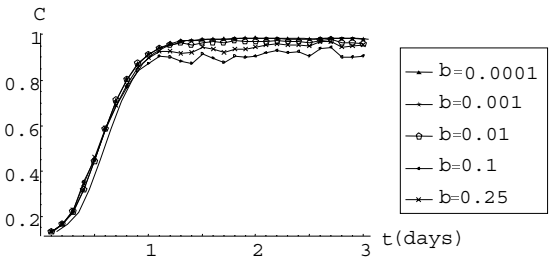

Figure 4. Concentration profile at *x* = 0.5m for σ^2 = 0.001.

One can expect to see the increase of stochasticity with the increase of correlation length. When *b* is very small, flow is smooth and stable. However, it is interesting to see that, *b* at 0.1m makes the concentration profile more variable. When *b* at higher regime, 0.25m for example, the flow is less stochastic than it was at 0.1m. This may cause by a sensitive range of *b* around 0.01 m. Figure 5 shows the concentration breakthrough curves for the similar *b* ranges at σ^2 =0.01. Flow tends to be unsteady for larger correlation lengths; however, stochasticity of smaller *b* values is still trivial. Increase of σ^2 intensifies stochasticity and effect of *b* in the flow a great deal. The unpredictable behaviour of the flow around 0.01 m of *b* shown in Figure 4 exists in current σ^2 as well.

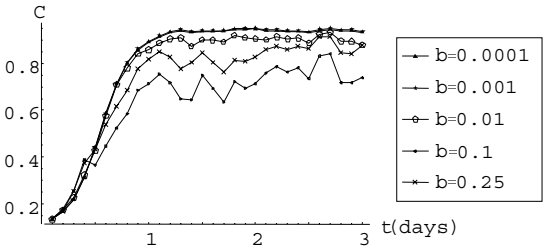

Figure 5. Concentration profile at x = 0.5m for σ^2 = 0.01.

We extended the investigation by keeping b at a constant and changing σ^2. Figure 6 shows the concentration profiles at b = 0.0001 for varying σ^2 (0.0001 to 0.25). In Figure 3, small σ^2 demonstrates negligible stochasticity even for very high b values, whereas, in Figure 6, irrespective of smaller b, σ^2 influences the stochasticity of the flow. However, it is difficult to distinguish the concentration profiles for smaller σ^2 (0.0001 and 0.001). With the increase of σ^2 stochasticity increases rapidly. Therefore, we can assume that σ^2 is the dominant parameter which regulates the behaviour of the flow.

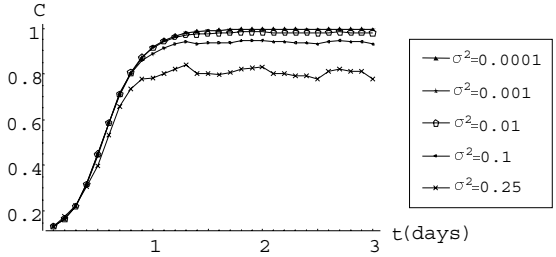

Figure 6. Concentration profile at x = 0.5m for b = 0.0001.

We increased b by 10 times and obtained Figure 7 which shows that stochasticity increases considerably.

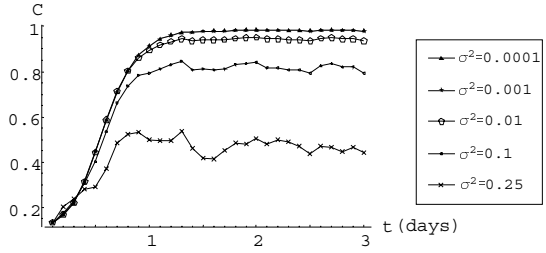

Figure 7. Concentration profile at x = 0.5m for b = 0.001.

It may be more appropriate and statistically sound to use confidence intervals rather than depend on a few realisations of standard Wiener increments to understand the effect of σ^2. We used 50 different Wiener increments to calculate the 95% confidence intervals. Figure 8(a) clearly shows that for smaller values of parameters (σ^2 =0.001, b= 0.01), which represent less heterogeneity of the system, variation of concentration profile is negligible and hardly distinguishable. Figure 8(b) exhibits that when parameter values are increased the stochasticity inflates. The confidence intervals of Figure 8(b) demonstrate that the model is quite stable even for highly stochastic flow.

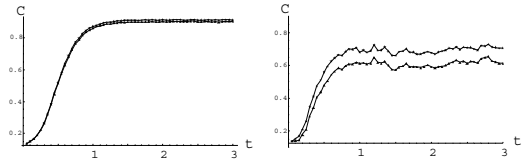

(a) (b)

Figure 8. 95% of confidence interval profiles with 50 different Wiener increments; (a) σ^2 =0.001, b=0.01 (b) σ^2 =0.1, b= 0.1.

We explored the effect of different random Wiener process increments. Figure 9 and 10 show the concentration profiles for five different Wiener processes for two different combinations of parameters. There is no considerable difference among these breakthrough curves, i.e. the influence of the Wiener process is minimal to the nature of the flow.

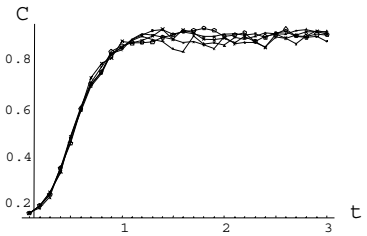

Figure 9. Concentration profiles for five different Wiener process increments at x = 0.5m for σ^2 = 0.001 and b=0.01.

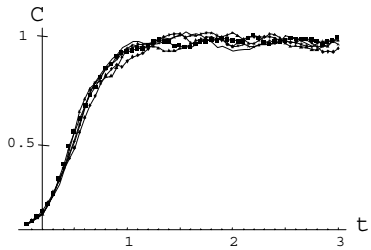

Figure 10. Concentration profiles for five different Wiener process increments at x = 0.5m for σ^2 = 0.01 and b=0.1.

3.1 Hypotheses

Having understood some of the features of the model behaviour, we can develop hypotheses about the parameters of the stochastic model

relating to the physical phenomenon. It was hypothesised that the variance, σ^2, is a function of pore size and inversely proportional to the porosity ($\sigma^2 \propto (1/\varphi)$, where φ = porosity). Low σ^2 represents larger pore size and more possible travel paths, i.e. solute can travel with water with fewer disturbances in less heterogeneous media. As a result, randomness of the travel paths and the occurrence of random mixing decrease. On other hand, larger σ^2 represents a medium of smaller pore size. Therefore, there are less straight travel paths and water tends to travel in various directions. This phenomenon can increase the mixing of the solute and, hence, increases dispersion and stochasticity.

We further hypothesised that the correlation length, *b* is representative of the geometry of the pores. The small *b* represents the medium of isotropic and homogeneous formation, and larger *b* represents anistropic and heterogeneous porous medium.

When the pore sizes are fairly large the effect of the geometry is negligible. Flow paths can find easier ways through larger pores irrespective of the shapes of particles. Figure 3 shows that hypotheses are reasonable. Low σ^2, 0.0001, represents large pores, therefore the flow is stable for all the shapes of geometry (any *b* value). In the case of larger σ^2, where pore size is smaller, the geometry can play a vital role. Even though the effective pore size is smaller, if geometry of the pores are regular, particles could find a reasonably homogeneous paths and that comparatively reduces the random mixing of flow (Figure 4 and 5). In addition, the geometry and size of pores are interrelated in a complex manner.

We investigated the effect of parameters for larger scales: 10 m, 20 m, 30 m, 50 m and 100 m. Figure 11 and Figure 12 show that increase of stochasticity with the σ^2 for 10 m domain. Comparison of Figure 11 and Figure 13 illustrate

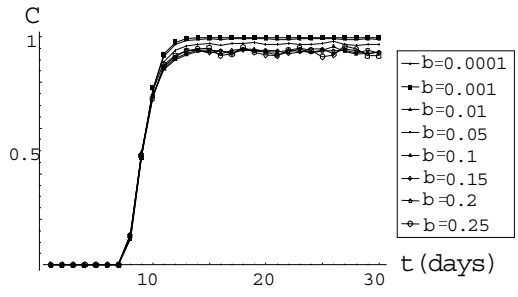

Figure 11. Concentration profile at *x* = 5m (of 10 m domain) for σ^2 = 0.0001

that σ^2 is the most dominant parameter and our hypotheses are valid for larger scales as well.

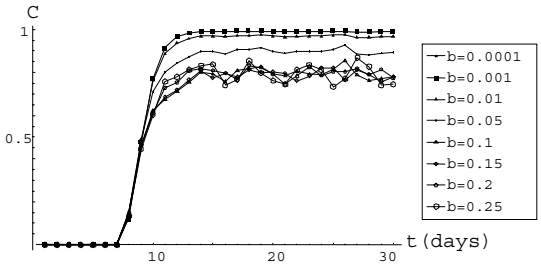

Figure 12. Concentration profile at *x* = 5m (of 10 m domain) for σ^2 = 0.001

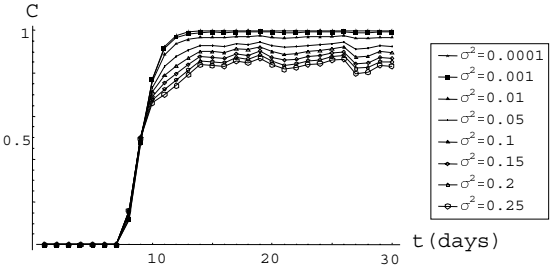

Figure 13. Concentration profile at *x* = 5m (of 10 m domain) for b = 0.0001

3.2 Scale Dependency

As the use of a dispersion coefficient, *D*, was avoided in the formulation of SSTM, the scale affect of *D* would not affect the model solution. Therefore, it is important to investigate whether the model could capture the scale effect in representing stochastic flow.

Comparison of Figure 3 and Figure 11 shows that stochasticity of the flow has increased with the scale for similar parameters. Figure 4 and Figure 12, Figure 6 and Figure 13 illustrate the same. Figure 3, 11 and 14 demonstrate that the rate of increase of stochasticity is decreasing with scale. Even though similar model performances are evident in other scales, visual comparison may not be sufficient to conclusively support capturing of scale dependency. Therefore, we investigated the ways of estimating *D* to recognise the increase of stochasticity with scale. We employed the stochastic inverse method mentioned earlier to estimate *D* by using concentration realisations of SSTM [Rajanayaka et al., 2001]. As Figure 1 and Figure 2 show, *D* has increased from 0.01 m^2/day to 0.037 m^2/day with the scale for same parameters. However, Rajanayaka et al. [2001] showed that the reliability of the estimates obtained from the stochastic estimation method reduces with the increase of stochasticity.

Therefore, such estimation method may not be suitable to estimate parameters with highly stochastic flows where values of σ^2 and b are large. However, flow with low level stochasticity illustrates SSTM is capable of capturing the scale dependency of D.

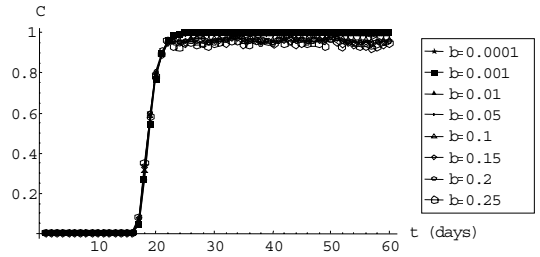

Figure 14. Concentration profile at x = 10m (of 20 m domain) for $\sigma^2 = 0.0001$

4. CONCLUSIONS

In this paper, we investigated a stochastic model to understand its statistical behaviour for different model parameter values. The correlation length, b, and the variance, σ^2, are the main parameters of the model. The model mimics the advection-dispersion solution with a greater accuracy provided appropriate parameters are selected. It was found that the two parameters influence the flow in a complex manner and there is a correlation between two parameters. However, σ^2 is more dominant and determines the stochasticity of the flow. We hypothesised that σ^2 is inversely proportional to the pore size and b represents the geometry of the pores; smaller b represents isotropic and homogeneous media, and lager b characterises the anisotropic and heterogeneous medium. The flow profiles of different scales, 1 m – 100 m, demonstrate that our hypotheses are reasonable. In addition, computational results show that SSTM could capture the scale dependence of the dispersion flow, however, the rate of increase of stochasticity tends to decrease with the scale. Since, the accuracy of the estimates given by the stochastic inverse parameter estimation method, which was employed to obtain D, reduces at high stochasticity, it was difficult to conclusively determine the nature of the scale dependency. The model was stable and robust when tested with different realisations of the standard Wiener processes and confidence intervals.

5. REFERENCE

Dagan, G., Solute transport in heterogeneous porous formations. *Journal of fluid mechanics*, *145*: 151-177, 1984.

Dagan, G., Time dependent macrodispersion for solute transport in anisotropic heterogeneous aquifers. *Water Research Resource, 24*(9): 1491-1500, 1988.

Fetter. C. W., *Contaminant Hydrogeology*, Prentice-Hall Inc., New Jersey, 1999.

Foussereau, X., W.D. Graham, G. Ashie Akpoji, G. Destouni, and P.S.C. Rao, Stochastic analysis of transport in unsaturated heterogeneous soils under transient flow regimes. *Water Research Resource, 36*(4): 911-921, 2000.

Freeze, R.A., A stochastic-conceptual analysis of one dimensional groundwater flow in a non-uniform homogeneous media. *Water Research Resource, 11*(5): 725-741, 1975.

Gelhar, L. W., A.L. Gutjahr and R.L. Naff, Stochastic analysis of microdispersion in a stratified aquifer. *Water Research Resource, 15*(6): 1387-1391, 1979.

Gelhar, L. W., Stochastic subsurface hydrology from theory to applications. *Water Research Resource, 22*(9): 135S-145S, 1986.

Kulasiri, D. and W.S. Verwoerd, A stochastic model for solute transport in porous media: mathematical basis and computational solution, Proc. MODSIM 1999 International congress on modelling and simulation, Hamilton, New Zealand; 31-36, 1999.

Kulasiri, D. and W.S. Verwoerd, Stochastic dynamics of solute transport in porous media, volume 1, Research monograph (89 pages), Centre for Advanced Computational Solutions (C-fACS), Lincoln University, New Zealand, 2001.

Neuman, S. P., C.L. Winter and C.N. Neuman, Stochastic theory of field scale Fickian dispersion in anisotropic porous media. *Water Research Resource, 23*(3): 453-466, 1987.

Rajanayaka, C. and D. Kulasiri, Investigation of a stochastic inverse method to estimate parameters in groundwater models, Proc. MODSIM 2001 International congress on modelling and simulation, Canberra, Australia; 1985 – 1990, 2001.

Russo, D., Stoshastic modelling of microdispersion for solute transport in a heterogeneous unsaturated porous formation, *Water Research Resource, 29*: 383-397, 1993.

Unny, T.E., Stochastic partial differential equations in groundwater hydrology – Part 1: *Journal Hydrology and Hydraulics; 3*:135-153, 1989.